A zero-sequence impedance-based fault location method for MV distribution feeders with sparse measurements

Alexandre Bach, T. -D. Le, Marc Petit

A ZERO-SEQUENCE IMPEDANCE-BASED FAULT LOCATION METHOD FOR MV DISTRIBUTION FEEDERS WITH SPARSE MEASUREMENTS

Alexandre Bach[1*], Trung-Dung Le[1], Marc Petit[1]

[1] Université Paris-Saclay, CentraleSupelec, CNRS, Laboratoire de Génie Electrique et Electronique de Paris, 91192, Gif-sur-Yvette, France.
Sorbonne Université, CNRS, Laboratoire de Génie Electrique et Electronique de Paris, 75252, Paris, France
**alexandre.bach@centralesupelec.fr*

Keywords: FAULT LOCATION, IMPEDANCE-BASED METHOD, DISTRIBUTION FEEDERS, SPARSE MEASUREMENT, PHASOR MEASUREMENT UNITS

Abstract

This paper presents a fault location method developed for medium voltage (MV) radial distribution feeders using zero-sequence components and a limited number of measurement nodes. The method exhibits promising results in simulation with unsynchronized measurements and can be further enhanced with the use of synchronized measurements such as the ones coming from phasor measurement units (PMUs). Using synchronized measurements, the method has been able to reach its full locating potential on all simulated faults occurring on the most challenging distribution feeder reconstructed. Finally, the presented method is cost effective since the fault is located with only voltage measurements on all the chosen secondary substations and can locate all types of earth faults.

1 Introduction

In presence of a fault on a distribution feeder, the DSO needs to locate the fault as quickly and as precisely as possible. Indeed, the fault clearing time, hence the cost of lost load, is highly correlated to the ability of maintenance teams to restore the grid to the nominal operating conditions. Usually, measurements are only performed at the primary substation, leading to major limitations for impedance-based fault location methods, such as multiple locations. With the rise of smart grids, additional measurement units might be installed in some secondary substations on MV feeders, as some DSOs already experimented [1].

Most of the proposed fault location methods are divided into two categories. First, impedance-based methods rely on the fundamental components of measured voltages and currents. They are said to be cost-efficient but present the problem of multiple locations [2][3]. It is indeed not possible to differentiate between two nodes located at the same electrical distance of a given measurement node. Secondly, transient-based methods rely on the measure or estimation of the propagating time of the wave resulting from the apparition of the fault. Different estimators based on time reversal similarity [4], wavelets [5] and others give the fault location estimation. Such methods might be more accurate than the others at the expense of a need for a very high sampling rate due to the high propagation speed of the wave. There are still very few measurement devices deployed on the grid which are compliant with this requirement. That is why this paper presents an impedance-based FLM with additional measurements along MV feeders, which can be deployed using the current generation of sensors usually used by DSOs.

[6] shows that the 2 voltage estimates along a transmission line with measurements installed at both extremities are equal on the fault position. In order to apply such idea on a MV feeder, and not only on a 2 buses system, there is a need for the value of the load current at each injection node. Most for the impedance-based FLMs need for the values of load current at every substation to perform as expected, which is one of the most limiting factor. Unfortunately, a DSO does not usually dispose of such information. That is why [7] developed a FLM using the negative sequence components, arguing that the value of load current is negligeable in the negative sequence. However, real data obtained from Enedis at the distribution level have shown a negative-sequence current ratio in the healthy feeder which are neighbours of a fault ranging from 15.9% up to 39.6%. Given that load current in the faulty feeder should behave the same way as the current in the healthy feeders, the hypothesis seems too strong. This led us to think that considering that load currents have no negative sequence component is not a viable hypothesis at the distribution level. Moreover, 0-sequence impedance values stored in DSO databases should be good estimates of the real ones, since errors committed in the estimation of 0-sequence line impedances values due to incorrect estimation of earth resistivity, which [7] present as too important at the transmission level, have a smaller impact. Given the fact that a large majority of transformers in primary and secondary substations have one of their windings which is Delta-coupled, 0-sequence currents cannot pass from one voltage level to another. That is why knowing line impedances and 0-sequence

voltage and current at the primary substation is enough to compute 0-sequence voltage and current in all the nodes of the feeder when sound, without a need for load current values. Based on this fact, a 0-sequence FLM has been developed.

To overcome the multiple estimation problem encountered with impedance-based methods, there is a need for multiple measurement nodes in a given feeder [8]. In the literature, most of the FLMs are focusing on the observability of the voltage along the feeder and rely on the "1-bus spacement method" [9][10] which needs a very high number of measurement nodes: from 10% up to 35% of the nodes need to be instrumented. This represents an investment of hundreds of sensors for a long rural feeder, which is too costly with respect to the added value it leads to. While the presented method does not enable the DSO to perform state estimation, which is possible using the 1-bus spacement method, it can obtain a set of nodes near the fault forming a solution area which size can be known a priori with a very low number of additional measurements.

This paper presents an overview of the developed methods for fault location and for the optimal placement of additional measurements. Then, it shows results from simulations using the CIGRE MV distribution network benchmark (CIGRE network) and using a distribution feeder built from the open database of the French distribution system operator (DSO) Enedis.

2 Presentation of the method

2.1 The fault location method

The fault location method is based on the estimation of the 0-sequence voltages along the path from the primary substation to each of the measurement nodes (Top-Down estimation) and vice-versa (Bottom-Up estimation). Given the fact that the fault location is unknown, only the 0-sequence line impedance values are used in the estimation process. A PI lumped-parameters model of the lines, including 0-sequence serial resistance, serial reactance and parallel capacitance is used since they are the parameters stored by DSOs in their database to describe a feeder. Fig. 1 represents the equivalent 0-sequence impedance between node k and node m, which leads to the way of computing 0-sequence voltages and currents from one node to another one following a path, given by (1):

$$\begin{pmatrix} V_0^m \\ i_0^m \end{pmatrix} = \begin{pmatrix} 1 + \frac{Z_0^{lig}}{Z_0^k} & Z_0^{lig} \\ -\frac{1}{Z_0^k} - \frac{1}{Z_0^m} - \frac{Z_0^{lig}}{Z_0^k Z_0^m} & -1 - \frac{Z_0^{lig}}{Z_0^m} \end{pmatrix} \begin{pmatrix} V_0^k \\ -i_0^k \end{pmatrix} \quad (1)$$

The estimation process is done without supposing a location for the fault, as if the feeder was sound, with the only knowledge of 0-sequence line impedances values. Fig. 2 exhibits the behaviour of the algorithm on the first feeder of the CIGRE network [2] considering an earth fault occurring at node 10 and considering the path between the busbar and the first measurement node: node 6. This means that for the Top-Down estimation, the currents measured at the beginning of the faulty feeder are used for the computation of the voltage drops along the path (15 to 6 in Fig. 2), and not only for the nodes along the fault path (15 to 3). So, the voltage drops computed correspond to the real voltage drops induced by the fault for nodes in the fault path (15 to 3) while the computed voltage drops are inaccurate for the other nodes (4 to 6) since only a capacitive current is flowing, as shown in Fig. 2(a). Symmetrically, when computing the voltage drops in the Bottom-Up estimation process, only capacitive current is considered since the fault position is not known and no 0-sequence current can be measured in Delta-coupled windings in the secondary substations. This leads to erroneous voltage drops estimations on the nodes in the fault path (15 to 2), where there is a faulty current which is not taken into account, while the voltage drops estimates will be accurate for the other nodes (3 to 6) where only capacitive current is flowing as shown in Fig. 2(b).

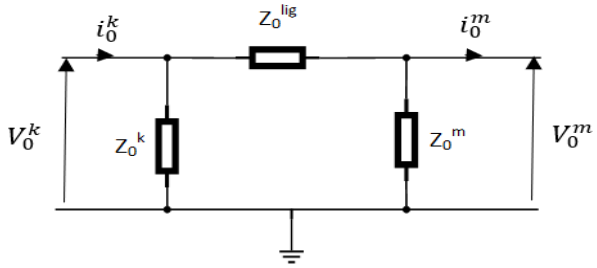

Fig. 1: PI lumped-parameters 0-sequence model of a line

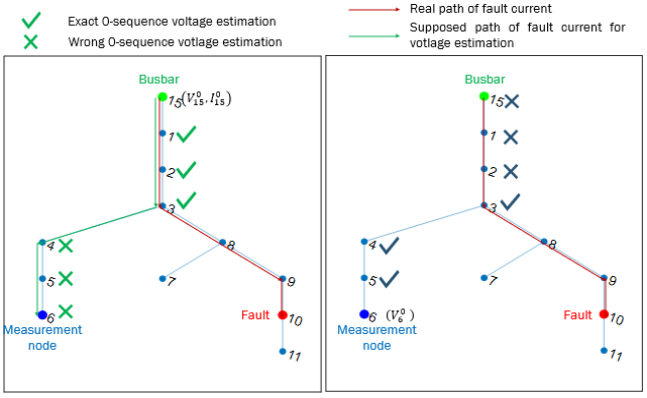

(a) (b)

Fig. 2: Example of the FLM on the CIGRE network with (a) Top-Down and (b) Bottom-Up estimation from busbar to 6

As a result, for a given path from the primary substation to a measurement node (Top-Down), the voltage estimates will be accurate for the nodes which are along the fault path, and inaccurate outside. Symmetrically, the estimates computed from each secondary measurement nodes (Bottom-Up) will be inaccurate for the nodes along the fault path since it does not consider the existence of a fault. The two sets of voltage estimates are equal on the node which is the nearest to the fault and on the path between the two considered measurements. It is called the projection node (ProjectNode) in Fig. 3. To obtain such node, there is a need to compare the values of 0-sequence voltages along the path between the 2 sets of estimates and search for the position of the minimum difference. If the

measurements are synchronized together, as when using PMUs, the difference of the phasors can be performed while only difference of magnitudes is performed when using unsynchronized measurements.

For a given path between the busbar and a measurement node (path 15 to 6 in Fig. 2), the projection node enables to set a lateral branch that is defined as the set of nodes being downstream to the projection node but outside the path under study (path 15 to 6). In Fig. 2, the lateral branch of node 3 with respect to the path 15 to 6 is the set of nodes $\Omega_6 = \{3,8,7,9,10,11\}$. If a fault occurs in any of these nodes, the FLM would give the same answer, i.e. the projection node is the node 3. For a given feeder with M additional measurements at secondary substations, the method should give M sets of lateral branches $\Omega_i, i \in [\![1, M]\!]$ which are the lateral branches of each projection node N_i with respect to each path. It is not possible to locate the fault more precisely inside this set without adding another measurement. By using M additional measurements optimally placed, the most likely area for the fault location is obtained by (2). The total length of the lines inside of Ω_{sol}^{M} can be known a priori, so that the number of additional measurements can be chosen to have a size compatible with the DSO needs.

$$\Omega_{sol}^{M} = \cap_{i=1}^{M} \Omega_i \tag{2}$$

Algorithm 1: Fault Location Method

When an earth fault is located

Data:

AdditionalMeas ; /* List of M additional measurements */

V_0; /* 0-sequence voltage measurements */

Z_0; /* 0-sequence impedance matrix */

for *i=1 to M* /* for all M additional measurements */

  $\Omega_i = \varnothing$

  for *k=1 to K* /* for all K nodes from busbar to j */

    $V_0^{top-down}(k)$=UpstreamVoltageEstimation($V_0(i)$,$V_0(busbar)$,Z_0)

    $V_0^{bottom-up}(k)$=DownstreamVoltageEstimation($V_0(busbar)$,$V_0(i)$,Z_0)

  end

  if *Synchronised measurements* **then** /* using PMUs */

    ProjectNode=$\underset{k}{\operatorname{argmin}}(|V_0^{top-down}(k) - V_0^{bottom-up}(k)|)$

  else

    ProjectNode=$\underset{k}{\operatorname{argmin}}(||V_0^{top-down}(k)| - |V_0^{bottom-up}(k)||)$

  end

  LateralNodes=ListLateralNodes(ProjectNode,AdditionalMeas);

  /* List of X lateral nodes solution */

  $\Omega_i = \bigcup_{x=1}^{X} LateralNodes(x)$

end

return Ω_i

Fig. 3: Pseudo-code presenting the FLM

The robustness of the method can be increased by setting a margin of m measurements so that the fault location area is composed of the set of nodes located M-m times in a solution area: $\Omega_{sol}^{M-m} = \cap_{i=1}^{M-m} \Omega_i$. The margin m enables the algorithm to perform as expected theoretically when using M-m additional measurements even if there are m misfunctioning ones.

2.2 Location of the additional measurements

Since the performance of the method depends on to the good positioning of the additional measurements in secondary substations, an optimal placement method has been developed based on a performance index for the FLM. Since this FLM cannot discriminate the nodes inside Ω_{sol}^{M} for M additional measurements, the FLM does not necessarily provide us with a single estimation of the fault location. The most usually found performance index for FLMs in the literature is the distance between the true fault location and the estimated one. This index cannot be used to quantify the performance of this FLM since there is not a unique fault location estimation. Given that this FLM gives an area in which the fault is the most likely to be, noted Ω_{sol}^{M} for M additional measurements, the performance of the FLM is as high as the total length of the lines in the area is small. Indeed, it is correlated to the time required for a maintenance team to travel across the solution area in search for the fault. To discriminate between two sets of additional measurements, we define the probability of a fault to occur at node j as $FP(j)$ and the length of the solution area as $L_{sol}(j)$. $L_{sol}(j)$ is defined by (3) where – for a given set of M additional measurements – $\Omega_{sol}^{M}(j)$ is computed for a fault located on the node j and the sum of the length of all lines inside $\Omega_{sol}^{M}(j)$ is computed

$$L_{sol}(j) = \sum_{k \in \Omega_{sol}^{M}(j)} L(k) \tag{3}$$

$$\mathbb{E}[L_{sol}] = \sum_{j \in nodes} L_{sol}(j) FP(j) \tag{4}$$

Three fault probability density functions (PDF) have been tested. First, a uniform probability on all nodes was chosen. Giving the fact that a common assumption is to consider that the probability of fault is uniform along a line, this fault probability does not behaves as wanted. Indeed, a set of nodes close from each other would have the same fault probability than a set of nodes very far from each other, thus representing higher value of lines length. That is why this fault probability has not been investigated in this paper. The second fault probability considered is a uniform distribution with the length of the lines. This type of probability does not consider the fact that underground cables are far less subjected to faults than overhead lines (OHL). As shown in [11], the 1991 statistics in France show that the fault probability is 13 times higher on OHLs than on underground cables. That is why a third fault probability with a 10 times higher fault probability on OHLs has been tested.

Then, an optimal placement method has been developed. The way the FLM estimates the fault location makes the remote ends of the feeder the best candidates to place additional measurements. Indeed, an additional measurement placed downstream to another one should give the same information when the fault is upstream of both and more if it is not the case. That is why the optimal placement algorithm searches iteratively for the best additional measurement node to add from the secondary substations that are at the extremities of the feeder so that $\mathbb{E}[L_{solution}]$ is minimized, as introduced by (4) and shown in Fig. 4. The value of the fault probability at every node $FP(j)$ and the current set of additional measurements are needed to search for the optimal new one. For every node j and

every possible configuration, the theoretical length of the solution area associated to a fault at node j, noted $L_{sol}(j)$ is computed, enabling us to compute $\mathbb{E}[L_{solution}]$.

Algorithm 2: Optimal placement method

Data:
AdditionalMeas ; /* List of additional measurements */
FP; /* Fault probability at every node */
for *i=1 to M* /* for all M substations at extremity remaining */
  NewAdditionalMeas=Union(AdditionalMeas,i)
  for *j=1 to N* /* for all N nodes */
    $L_{sol}(i,j)$=computeLsol(NewAdditionalMeas)
  end
  $\mathbb{E}[L_{sol}](i) = \sum_{j=1}^{N}[FaultProbability(j) * L_{sol}(i,j)]$
end
NextMeasurement=$arg\min_i(\mathbb{E}[L_{sol}](i))$
return NextMeasurement

Fig. 4: Pseudo-code of the optimal placement algorithm

Fig. 5 presents the topology of the considered feeder in the next part, which is the longest and most ramified one from the database, representing the most challenging case for the FLM. OHLs are represented in dark red while underground cables are in bright blue. Large section OHLs and cables (with $r_d \leq 0.4\ \Omega.km^{-1}$ corresponding to a section bigger than $80\ mm^2$) are thick while small section lines are thin. The optimal order of placement of additional measurements is shown with the black nodes having a label, so that a DSO who would want to equip M secondary substations with additional voltage measurements should equip the ones labelled from 1 to M. Fig. 5 shows the placement priority considering the second fault probability which is based on the length of the lines only. As expected, the first needed measurement location is one of the farthest away substations from the busbar, since it provides the longest path of nodes, forming the main artery, for which the location is exact. Then, the other substations on which putting an additional measurement would be efficient are located at the end of the longest lateral branches to this main artery.

For example, we can see that the second most needed additional measurement for the second fault PDF is at the end of an underground branch. When using the third fault portability, which is the closest to the reality, this node does not appear in the 7 most needed additional measurements. Meaning that a DSO can save some measurement devices where there is a lot of underground cables since it has a lower fault probability or can deploy them in another branch where they should prove more useful. The FLM can cover a very high part of the feeder with a rather small set of additional measurements compared to the methods found in the literature. Indeed, with very sparse measurements, it can locate exactly a fault for all points on a path between the busbar and one instrumented substation while having an area of location for the lateral nodes.

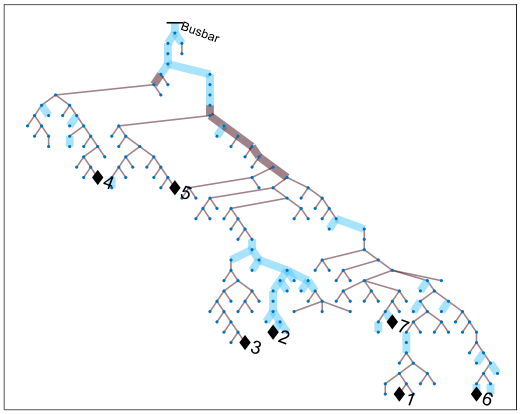

Fig. 5: Feeder topology and 7 first placement priority considering the second fault PDF

3 Simulation results

3.1 CIGRE MV distribution network benchmark

The FLM has been tested in simulation using MATLAB Simulink to assess its performances. The FLM has been tested first on a modified version of the CIGRE network with 3 additional measurements: one on each of the feeder's ends at nodes 6,7 and 11, as represented in Fig. 2, representing the best-case scenario for this FLM. The main characteristics of this feeder are its total length $L_{tot} = 29.32\ km$, being the sum of the length of all lines in the feeder, its total load power $P_{tot} = 5.3$ MW and $Q_{tot} = 1.8$ MVAr and its distance between the most remote node and the busbar $L_{remote} = 21.06\ km$. This leads us to define a ramification index in (5), which value for this feeder is too weak to represent the complexity of some rural feeders.

$$ram = \frac{L_{tot}}{L_{remote}} = 1.39 \quad (5)$$

The FLM has first been tested on a single-phase fault, representing more than 75% of the faults according to the French DSO [11]. We simulated an A-G fault at node 10 with fault impedance $R_f = 150\ \Omega$ which is higher than the observed fault impedances in 90% of the cases. The magnitude of the 0-sequence voltage estimates at each node along the path between the busbar 15 and the first measurement 6 is shown in Fig. 6. Given that the fault is located at node 10, the two sets of voltage estimates should be equal at node 3 since node 10 is in the lateral branch of node 3 with respect to this path. We observe that the algorithm is behaving as expected for this fault. The intersection of the solution areas from the 3 additional measurements gives in the exact location of the fault (6):

$$\Omega_{sol}^{3} = \Omega_6 \cap \Omega_7 \cap \Omega_{11} = \{10\} \quad (6)$$

The fault was accurately located with unsynchronized or synchronized measurements. However, using synchronized measurement makes the FLM more robust since we observe

greater margin in the difference of estimates, defined for every node i in the path as $\Delta V_0^i = \left|V_0^{i,top-down} - V_0^{i,bottom-up}\right|$, considering the phasor values $\left|V_0^{i,top-down}\right|\angle V_0^{i,top-down}$ with synchronized measurements or only the magnitude values $\left|V_0^{i,top-down}\right|$ without any phase reference.

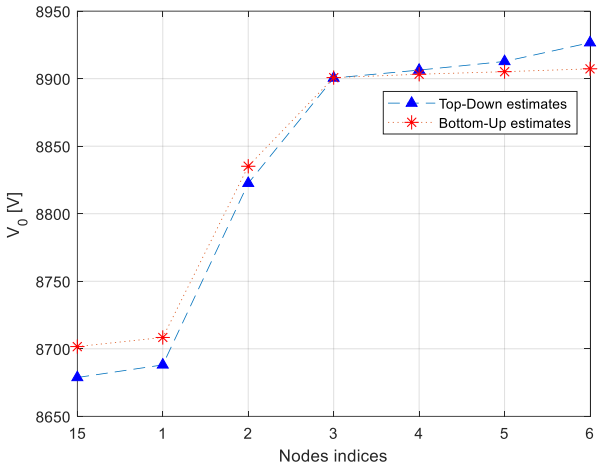

Fig. 6: 0-sequence voltage estimates from busbar 15 to 6

Indeed, Fig. 7 shows that using the information given by the phase results in greater differences between the two sets of estimates, making the identification of the projection node easier and more robust since the difference of estimates in some nodes of the path goes from 20V without synchronization up to 70V with synchronized measurements considering the same simulation.

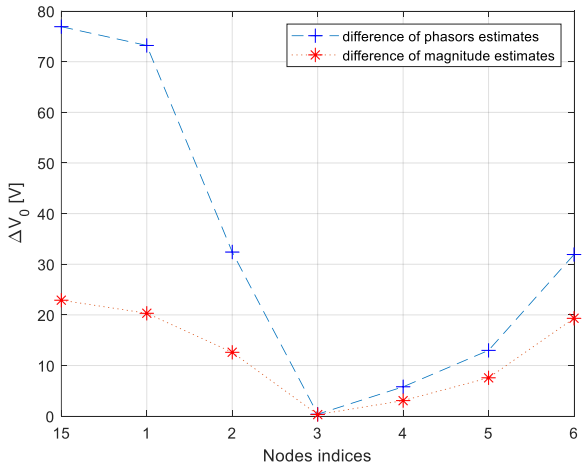

Fig. 7: difference of estimates with/without synchronization

3.2 Reconstruction of real feeders from Enedis Open Data

In the Appendix B of [12], 20 feeders from a French HV/MV substation have been built using the open data of Enedis. This provided us with feeder topologies, including line impedance values and load values, enabling us to modify the vanilla version of the CIGRE network so that it becomes representative of an average real feeder. Indeed, the average values of total length and ramification index observed on these 20 feeders are $\langle L_{tot}\rangle = 20.26\ km$ and $\langle ram\rangle = 1.48$. However, this is not representative enough since some rural feeders have much more complex topologies with a much larger ramification index than the CIGRE network. So, there is a need to quantify the performances of the FLM on feeders which are closer to real complex rural feeders. The longest and most ramified of the 20 reconstructed feeders has been chosen to test the performances of the FLM. It is a 211 nodes feeder with the following characteristics: $L_{tot} = 75.05\ km$, $ram = 3.22$, $P_{load\ tot} = 4.18\ MW$ and $Q_{load\ tot} = 1.25\ MVAr$. The FLM has been implemented on the considered reconstructed feeder and shows promising results even with unsynchronized measurements while locating very precisely all type of earth faults when leveraging synchronization. It has been chosen to add the 4 most needed measurements obtained using the priority computed for this example; 4 measurements is considered to be an acceptable number for such long and ramified feeder. An A-G fault with fault resistance $R_f = 150\ \Omega$ in node 1043, called faulty node on Fig. 8, has been simulated on MATLAB Simulink. The faulty node is a node with high fault probability while being one of the worst-case scenarios for this set of additional measurements.

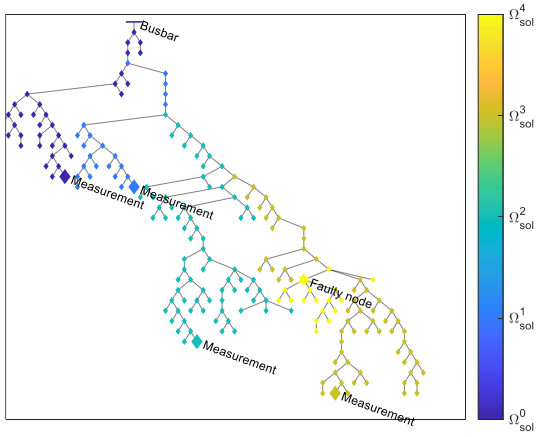

Fig. 8: Fault location area for synchronized measurements with colours related to the values of M-m

It appears that the downstream measurement, which corresponds to measurement 1 in previous part, is not able to locate correctly the projection node and the lateral branch without synchronization of the measurements. Indeed, the projection node of the faulty node on this path between the busbar and this measurement is the node 1055. Fig. 9 shows that the minimum of the difference of the two sets of estimates is reached at node 1058 when using unsynchronized measurements instead of node 1055. This results in Ω^4_{sol} being a set of two nodes near the fault but not containing it while the set of nodes being 3 times solution Ω^3_{sol} being here very large, as shown on Fig.8, meaning that taking a margin in the number of additional measurements used is not a viable solution here. However, using synchronized measurements is guaranteeing the expected behaviour of the FLM, as shown on Fig. 9, the projection node, being the node for which the difference of estimates is minimum, is the expected one. In this case, the

area of most likely nodes corresponds to the theoretical area we should obtain with the FLM, as shown in Fig. 8, meaning that the maximum locating potential of the FLM is reached. Fig. 8 represents the different areas Ω_{sol}^{M-m} considering the simulated fault and the M=4 chosen additional measurements. Using PMUs, the solution area is composed of 17 nodes, including the faulty one, which represents 5.05 km of lines being 6.7% of the feeder length, for one of the worst-case scenarios. For this fault, if the DSO would have chosen to equip 7 substations with measurements, the FLM would have been able to locate exactly the fault since measurement 7 is downstream of the faulty node.

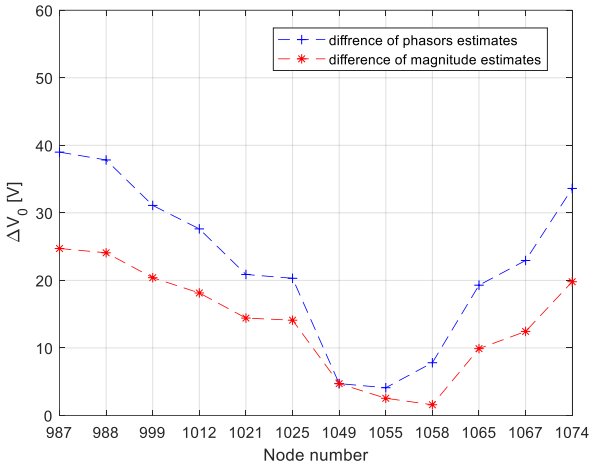

Fig. 9 : difference of estimates with or w/o synchronization

The deployment of PMUs at the distribution level on MV feeders could bring to DSO the possibility to use better FLM methods as the one presented in this paper is in need for synchronization to reach its full potential.

4 Conclusion

To conclude, it has been shown that the FLM developed can locate earth faults as precisely as wanted, providing that the number of additional measurements is high enough. Moreover, the FLM is in need of very sparse measurements since a small number is enough to obtain near the full location potential of the method, even on ramified feeders. It also appears that this method can take advantages of the increasing deployment of PMU in MV feeders since only data from synchronized measurements provide us with the optimal performances of the FLM on all tested faults. Next research around this method should focus first on the parametric study of the performances of the FLM considering variable fault positions and fault impedance values. Then, on the coupling between this method and other impedance based FLMs already deployed, such as Takagi-based [2], since it could enhance the location precision of both. Indeed, a Takagi-based FLM results generally in a set of different single nodes far from each other while the presented FLM generally gives an area of nodes but unique and around the faulty node. A coupling of such 2 methods could solve the problem of multiple estimation encountered by impedance-based FLMs while in need of only a few additional measurements with usual sampling frequencies values. Finally, there is a need to assess the optimal number of additional measurements and if the synchronization between them is needed for a given feeder. As shown, the performance of the method depends highly on the number of measurement nodes chosen and, on their synchronization. A technical-economical analysis will be carried out to be able to find out the optimal number of measurements with respect to their added-value for fault location.

5 References

[1] « VENTEEA Smart grid project », https://www.ademe.fr/sites/default/files/assets/documents/venteea.pdf, accessed 05 November 2021

[2] Le, T.D., M. Petit. « Earth fault location based on a Modified Takagi Method for MV distribution networks ». In *2016 IEEE International Energy Conference (ENERGYCON)*, 1-6, 2016.

[3] Liao, Y. « Fault Location for Single-Circuit Line Based on Bus-Impedance Matrix Utilizing Voltage Measurements ». *IEEE Transactions on Power Delivery* 23, nº 2 (April 2008): 609-17.

[4] Wang, Z., R. Razzaghi, M. Paolone, et al. « Electromagnetic Time Reversal Similarity Characteristics and Its Application to Locating Faults in Power Networks ». *IEEE Transactions on Power Delivery* 35, nº 4 (August 2020): 1735-48.

[5] Magnago, F.H., A. Abur. « Fault Location Using Wavelets ». *IEEE Transactions on Power Delivery* 13, nº 4 (October 1998): 1475-80.

[6] Silveira, E. G., C. Pereira. « Transmission Line Fault Location Using Two-Terminal Data Without Time Synchronization ». *IEEE Transactions on Power Systems* 22, nº 1 (February 2007): 498-99.

[7] Gong, Yanfeng, Mangapathirao Mynam, Armando Guzman, et al. « Automated Fault Location System for Nonhomogeneous Transmission Networks ». In *2012 65th Annual Conference for Protective Relay Engineers*, 374-81. College Station, TX, USA: IEEE, 2012.

[8] Garcia-Santander, L., P. Bastard, M. Petit, I. Gal, E. Lopez, et H. Opazo. « Down-Conductor Fault Detection and Location via a Voltage Based Method for Radial Distribution Networks ». IEE Proceedings - Generation, Transmission and Distribution 152, no 2 (2005): 180.

[9] Mazlumi, K., H. Askarian Abyaneh, S. H. H. Sadeghi, S. S. Geramian. « Determination of optimal PMU placement for fault-location observability ». In *2008 Third International Conference on Electric Utility Deregulation and Restructuring and Power Technologies*, 1938-42, 2008.

[10] Nuqui, R. F., A. G. Phadke. « Phasor measurement unit placement techniques for complete and incomplete observability ». *IEEE Transactions on Power Delivery* 20, nº 4 (October 2005): 2381-88.

[11] EDF GDF SERVICES. « Plan de protection des reseaux HTA, B.61-21: Principes ». In Guide technique de la distribution d'electricite, February 1994.

[12] Venegas, Felipe Gonzalez. « Electric Vehicle Integration into Distribution Systems: Considerations of User Behavior and Frameworks for Flexibility Implementation ». PhD thesis, Université Paris-Saclay, 2021.